Will be published:
Phys. Rev. Lett. 96, 230402 (2006)

arXiv:cond-mat/0601695v1 [cond-mat.mes-hall] 31 Jan 2006

Vortex-lattice melting in a one-dimensional optical lattice

Michiel Snoek and H. T. C. Stoof
Institute for Theoretical Physics, Utrecht University,
Leuvenlaan 4, 3584 CE Utrecht, The Netherlands

We investigate quantum fluctuations of a vortex lattice in a one-dimensional optical lattice. Our method gives full access to all the modes of the vortex lattice and we discuss in particular the Bloch bands of the Tkachenko modes. Because of the small number of particles in the pancake Bose-Einstein condensates at every site of the optical lattice, finite-size effects become very important. Therefore, the fluctuations in the vortex positions are inhomogeneous and the melting of the lattice occurs from the outside inwards. Tunneling between neighbouring pancakes substantially reduces the inhomogeneity as well as the size of the fluctuations.

PACS numbers: 03.75.Lm, 32.80.Pj, 67.40.-w, 67.40.Vs

Introduction. — Very rapidly rotating ultracold bosonic gases have been predicted to form highly-correlated quantum states [1, 2, 3]. In these states, the Bose-Einstein condensate has been completely depleted by quantum fluctuations, and quantum liquids appear with excitations that can carry fractional statistics. Some of these states have been identified with (bosonic) fractional quantum Hall states [2, 4, 5]. It is by now a long standing goal to observe the experimental signatures of these very interesting states in the context of ultracold quantum gases. The conditions for these states to form have been expressed in the requirement that the ratio $\nu = N/N_v$ of the number of atoms N and the number of vortices N_v, should be smaller than some critical value ν_c. The ratio ν plays the role of the filling factor and estimates for the critical ν_c are typically around 8 [2, 6]. These estimates are made for infinitely large systems.

However, observed filling factors are up till now always greater than 100, where almost perfect hexagonal lattices form and no sign of melting can be seen [7]. These experiments are carried out with Bose-Einstein condensates consisting of typically 10^5 particles, whereas the maximum number of vortices observed is around 300. Decreasing the number of particles results in loss of experimental signal, whereas the number of vortices is limited by the rotation frequency that has to be smaller than the transverse trapping frequency. Adding a quartic potential, which stabilizes the condensate also for rotation frequencies higher than the transverse trap frequency, has until now not improved this situation [8], although it has opened up the possibility of forming a giant vortex in the center of the cloud [9]. In recent work, however, it was realized that quantum fluctuations of the vortices can be greatly enhanced, without loosing experimental signal, by using a one-dimensional optical lattice [10]. The optical lattice divides the Bose-Einstein condensate into a stack of two-dimensional pancake condensates that are weakly coupled by tunneling as schematically shown in Fig. 1. The number of particles in a single pancake is much smaller than in a Bose-Einstein condensate in a harmonic trap, and therefore the fluctuations are much greater. Moreover, by varying the coupling between the pancakes, it is possible to study the dimensional crossover between decoupled two-dimensional melting, and the strong-coupling limit where the three-dimensional situation is recovered. Recently, the density profiles for quantum Hall liquids in such a geometry have also been calculated [11]. Because of the small number of particles in each pancake shaped Bose-Einstein condensate, finite-size effects become very pronounced in this setup. In particular, the critical filling factor for the melting of the lattice ν_c changes compared to the homogeneous situation. Moreover, melting is not expected to occur homogeneously but starts at the outside and then gradually moves inwards as the rotation speed increases. Therefore, phase coexistence is expected, where a vortex crystal is surrounded by a vortex liquid. In this Letter we study this interesting physics by investigating the quantum fluctuations of the vortex lattice for realistic numbers of particles and vortices. To decide whether or not the vortex lattice is melted we use the Lindemann criterion, which in this case has to be applied locally.

Besides the possibility of observing highly-correlated quantum states after the vortex lattice has melted, also the vortices themselves have very interesting properties. For moderately rotating gases, the vortices are observed to order in a Abrikosov lattice [12, 13]. The lowest mode

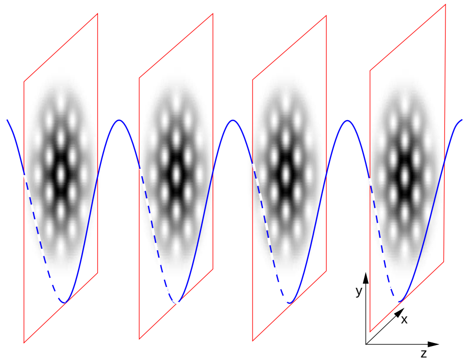

FIG. 1: (Color online) Setup in which the melting of the vortex lattice is studied. An optical lattice along the z-direction (indicated in blue) divides the condensate into pancake condensate which are coupled by tunneling processes.

of the lattice is the so-called Tkachenko mode [14], which recently has been investigated experimentally [7, 15] and theoretically [16, 17, 18]. Since the study of the fluctuations of the vortex lattice requires full information on all the modes of the lattice, we also can identify this mode. Because of the optical lattice, this mode actually becomes a Bloch band and we also determine the dispersion of the Tkachenko modes in the axial direction of the optical lattice.

Lattice vibrations. — The action describing the system in the rotating frame is given by $S = \int dt \int d^3\mathbf{x}\ \mathcal{L}(\mathbf{x}, t)$, with the Lagrange density given by

$$\mathcal{L} = \Psi^* \left(i\hbar\partial_t + \frac{\hbar^2 \nabla^2}{2m} - V(\mathbf{x}) + \Omega L_z - \frac{g}{2}|\Psi|^2 \right) \Psi, \quad (1)$$

where $\Psi(\mathbf{x}, t)$ is the Bose-Einstein condensate wavefunction, m is the mass of the atoms, Ω is the rotation frequency, $L_z = i\hbar(y\partial_x - x\partial y)$ is the angular momentum operator, and $g = 4\pi\hbar^2 a/m$ is the interaction strength, with a the three-dimensional scattering length. The combination of an optical lattice in the axial direction and harmonic confinement in the radial direction gives an external potential $V(\mathbf{x}) = V_z \cos^2(\lambda z/2) + \frac{1}{2}m\omega_\perp^2(x^2 + y^2)$, where λ is the wavelength of the laser producing the optical lattice. Assuming that the optical lattice is deep enough we can perform a tight-binding approximation and write $\Psi(\mathbf{x}, t) = \sum_i \Psi(z - z_i)\Psi_i(x, y, t)$, where $\Psi(z)$ is chosen to be the lowest Wannier function of the optical lattice. In this way we obtain the Lagrange density

$$\begin{aligned} \mathcal{L} = \sum_i \Psi_i^* (i\hbar\partial_t + \frac{\hbar^2\nabla^2}{2m} - \frac{m\omega_\perp^2}{2} r^2 + \Omega L_z - \frac{g'}{2}|\Psi_i|^2)\Psi_i \\ + t \sum_{\langle ij \rangle} \Psi_i^* \Psi_j, \qquad (2) \end{aligned}$$

where $\langle ij \rangle$ denotes that the sum is taken over nearest neighbouring sites. We have defined the interaction coefficient $g' = 4\pi\hbar^2 a/\sqrt{2\pi}\ell_z m$ and hopping amplitude $t = 4V_z^{3/4}E_z^{1/4}\exp[-2\sqrt{V_z/E_z}]$, where $E_z = 2\pi^2\hbar^2/\lambda^2 m$ is the recoil energy associated with the optical lattice and $l_z = \lambda/2\pi(V_z/E_z)^{1/4}$ is the harmonic length associated with the optical lattice.

Melting is only expected for a Bose-Einstein condensate that is weakly interacting. The wavefunction can then be taken to be part of the lowest Landau level. That is to say we consider wavefunctions of the form $\prod_i (z - z_i)\exp[-|z|^2/2]$, where $z = (x + iy)/\ell$, $z_i = (x_i + iy_i)/\ell$ and (x_i, y_i) is the position of the i^{th} vortex. Here ℓ is the 'magnetic length'. To increase the validity of this study, we use ℓ as a variational parameter instead of fixed it to the radial harmonic length, such that our results are also valid for stronger interactions [19]. The associated frequency is $\omega = \hbar/m\ell^2$. From now on distances are rescaled by ℓ, frequencies are scaled by the radial trappig frequency $\omega_\perp$, and we define a dimensionless interaction strength by means of $U = Ng'/4\pi\ell^2\hbar\omega_\perp = Na/\sqrt{2\pi}\ell_z$. In the calculations we take the scattering length of ^{87}Rb, $\lambda = 700$ nm and $V_z/E_z = 16$, which gives $U = 25N$. The on-site energy part of the Lagrange density depends in this approximation only on the particle density and becomes $(\omega + 1/\omega - 2\Omega)r^2 n(\mathbf{r})/2 + 2\pi\omega U n^2(\mathbf{r})$. The lowest Landau level wavefunctions and, therefore, also the atomic density, are fully determined by the location of the vortices. To consider the quantum mechanics of the vortex lattice we, therefore, replace the functional integral over the condensate wavefunctions by a path integral over the vortex positions.

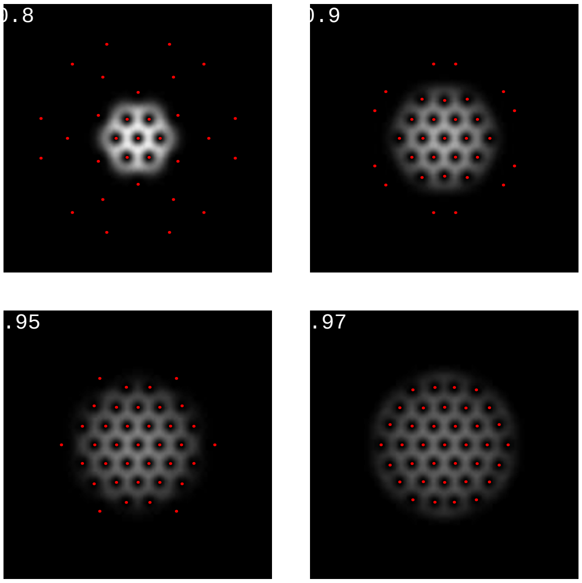

FIG. 2: (Color online) Classical vortex lattice and density profile for rotation frequencies $\Omega/\omega_\perp$ = .8, .9, .95 and .97. Here $U = 10$, which corresponds to $N = 250$. White means high density, black low density. The vortex positions are indicated by a red dot, such that also the vortices outside the condensate are visible.

Next we want to determine the quadratic fluctuations around the Abricosov lattice. To do so, we first have to find the classical groundstate. We calculated this groundstate for up to 37 vortices. For small numbers of vortices, the groundstate is distorted from the hexagonal lattice [21]. In general, there are also vortices far outside the condensate. The coarse-grained atomic density is well approximated by a Thomas-Fermi profile [22]. For fixed interaction U and different rotation frequencies pictures of the classical groundstate are given in Fig 2. Then we study the quadratic fluctuations by expanding the action up to second order in the fluctuations [20]. This yields an action of the form

$$S = \sum_i \mathbf{u}_i \cdot (\mathbf{T}i\partial_t - \mathbf{E}) \cdot \mathbf{u}_i - t \sum_{\langle ij \rangle} \mathbf{u}_i \cdot \mathbf{J} \cdot \mathbf{u}_j, \qquad (3)$$

where $\mathbf{u}_i = (\delta x_{1,i}, \delta y_{2,i}, \delta x_{2,i}, \delta y_{2,i}, \ldots) \equiv (\ldots, \mathbf{u}_{ni}, \ldots)$ is the total displacement vector of all the point vortices on site i, and $\mathbf{T}$, $\mathbf{E}$ and $\mathbf{J}$ are matrices depending on Ω, U, and the classical lattice positions. To diagonalize this action along the z-axis, we perform a Fourier transformation to obtain

$$S = \sum_k \mathbf{u}_k^* \cdot (\mathbf{T} i\partial_t - \mathbf{E} - t(1 - \cos[k\lambda/2]\mathbf{J}) \cdot \mathbf{u}_k \qquad (4)$$

Finally, we completely diagonalize this action by the transformation $\mathbf{v}_k = \mathbf{P}_k \mathbf{u}_k$ such that the action becomes $S = \sum_{k,\alpha} v_{k\alpha}^* (i\partial_t - \omega_\alpha(k)) v_{k\alpha}$ where $\omega_\alpha(k)$ are the mode frequencies of the vortex lattice. This means that the $v_{k\alpha}$, where k labels the momentum in the z-direction and α labels the mode, correspond to bosonic operators with commutation relation $[v_{k\alpha}, {v_{k'\alpha'}}^\dagger] = \delta_{kk'}\delta_{\alpha\alpha'}$. This allows us to calculate the expectation value for the fluctuations in the vortex positions, but also for the correlations between the various point vortices.

Tkachenko modes. — The Tkachenko modes are purely transverse modes of the vortex lattice. In a harmonic trap with spherical symmetry they become modes which are purely angular. In the radial direction their spectrum is discretized, because of the finite lattice size. The number of radial Tkachenko modes equals the number of vortex rings. For 37 vortices 6 Tkachenko modes can be identified. A close comparison with continuum theory for a finite-size system, where also a discrete spectrum was found [23], is possible but beyond the scope of this Letter. Moreover, the Tkachenko modes also have a dispersion in the z-direction. Without the optical lattice some aspects of these modes were recently investigated [24]. For typical parameters this dispersion is plotted in Fig. 3. As is clearly visible, there is one gapless mode, which is linear at long wavelengths, while the other modes are roughly just tight-binding like. Moreover, various avoided crossings between these modes are clearly visible. The gapless mode is the Goldstone mode associated with the spontaneously broken rotational $O(2)$-symmetry due to the presence of the vortex lattice. When the tunneling rate is very small, the gapped modes have exactly a tight-binding dispersion and the gapless mode gets a dispersion proportional to $\sin[k\lambda/2]$. This can be understood by observing that in this case the modes are decoupled and the Hamiltonian for the gapless mode reduces to the Josephson Hamiltonian $\mathcal{H} = -E_c \sum_i \partial^2/\partial\phi_i^2 + E_J \sum \cos(\phi_i - \phi_j)^2$, which indeed has this dispersion upon quadratic expansion.

It is interesting to note that for a small rotation frequency, which implies a small vortex lattice, the Tkachenko modes are not the lowest-lying modes. For $U = 10$, a Tkachenko mode becomes the lowest-lying gapped mode when $\Omega > .978$, but there are many modes in between the second and the third Tkachenko mode. This confirms the expectation that increasing the vortex lattice will bring down the Tkachenko spectrum more and more.

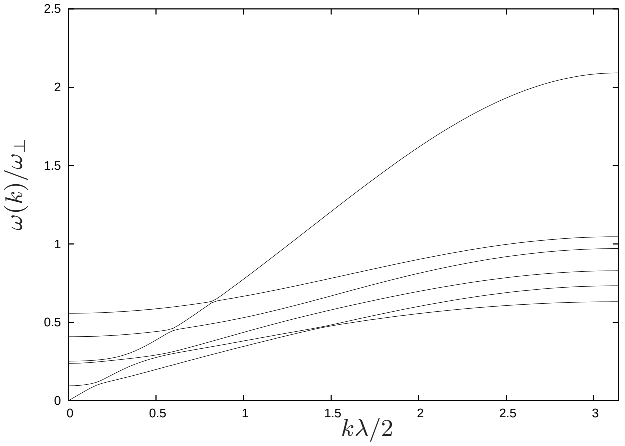

FIG. 3: Dispersion of the Tkachenko modes along the direction of the optical lattice. For this plot the parameters where chosen as: $U = 10$, $t = 1/10$, and $\Omega = .97$. One gapless linear mode and five gapped tight-binding like modes can be identified. The gapless mode is the acoustic Goldstone mode associated with the broken $O(2)$-symmetry due to the presence of the vortex lattice.

Vortex-lattice melting. — Quantum fluctuations of the vortices ultimately result in melting of the vortex lattice. To decide wether or not the lattice is melted, we use the Lindemann criterion, which in this inhomogeneous situation has to be applied locally. The Lindemann criterion means that the lattice is melted, when the ratio $\langle u_{ni}^2 \rangle / \Delta_{ni}^2$ of the displacement fluctuations of vortex n at site i and the square of the average distance to the neigbouring vortices Δ_{ni} exceeds a critical value c_L^2, which is known as the Lindemann parameter. For easy comparison with previous work on this topic, we use the value $c_L^2 = .02$. Because the coarse-grained particle density decreases with the distance to the origin, vortices on the outside are already melted, while the inner part of the crystal remains solid. Therefore a crystal phase in the inside coexists with a liquid phase on the outside. In Fig. 4 we compute the radius of the crystal phase $R_{\rm cr}$ normalized to the condensate radius R, as a function of the rotation frequency for fixed numbers of particles and an interaction strength U, and for various hopping strengths t. Here we define the condensate radius R as the radius for with the angularly averaged density drops below .003. The crystal radius $R_{\rm cr}$ is defined as the radius of the innermost vortex ring that is melted according to the Lindemann criterion. When according to this definition $R_{\rm cr} > R$, we set the crystal radius equal to the condensate radius, i.e., $R_{\rm cr} = R$. The ratio $R_{\rm cr}/R$ shows discrete steps because of the ring-like structure in which the vortices order themselves. We compare this with a simple local density calculation, where the criterion $N/N_v = n(r)/n_v(r) = 8$ derived in Ref. [6] is applied locally, using a Thomas-Fermi density profile to describe

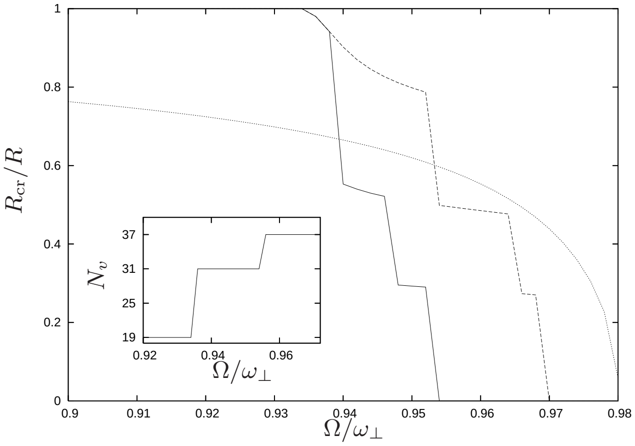

FIG. 4: Crystal radius $R_{\rm cr}$ normalized to the condensate radius R as a function of the rotation frequency for $N = 300$, $U = 10$. The full and dashed line are for $t = 0$ and $1/100$, respectively. The dotted line is the result of a local-density approximation. In the inset the number of vortices N_v that is within the condensate is plotted as a function of the rotation frequency.

the coarse-grained atomic density. From the on-site energy we extract that the variational parameter ℓ is set by the condition $\omega = \Omega$, and the Thomas-Fermi radius is given by $R^4 = 16\Omega^2 U/(1-\Omega^2)$. When taking a constant vortex density $n_v(r) = 1/\pi\ell^2$, the crystal radius normalized to the Thomas Fermi radius becomes $R_{\rm cr}/R_{\rm TF} = \sqrt{1-4R^2/N} = \sqrt{1-16/N\sqrt{\Omega^2 U/(1-\Omega^2)}}$. For comparison this line is plotted in Fig. 4. As expected for a finite system, the melting occurs considerably earlier than predicted by the local-density theory.

When the tunneling between pancakes is turned on, the fluctuations will also be coupled in the axial direction. This decreases the fluctuations in the vortex displacements because the stiffness of the vortices increases, and melting occurs for higher rotation frequencies, as is visible in Fig. 4. To determine the presence of crystalline order in the axial direction, we calculate $\langle e^{i\mathbf{q}\cdot(\mathbf{u}_{Ni}-\mathbf{u}_{nj})}\rangle$, which is related to the structure factor. For the central vortex we always find long-range order, while for the other vortices, we obtain an algebraic decay. This is in agreement with the expectation for a one-dimensional system at zero temperature. Note that the quantitative results in Fig. 4 depend on the value of the Lindemann parameter. Changing this value shifts the curves, but the qualitative features remain the same.

The liquid surrounding the crystal has rotational symmetry. Experimentally this can be observed, by noting that in the liquid the vortices are no longer individually visible, while in the crystal they are still visible, although their positions are broadened by the fluctuations. Theoretically it is a challenging problem to describe the coexisting crystal-liquid. This will allow to decide on the occurrence of melting based on energy considerations and thus shed more light on the accuracy of the application of the Lindemann criterion in this inhomogeneous situation. In the future we want to make a closer connection with continuum theory. Finally we want to extend the analysis to include a quartic potential, in which case giant vortex formation is prediction. In this case the liquid can also form in the center, instead of at the outer edge. Finally we also want to investigated the melting at nonzero temperatures, which is experimentally relevant, because the zero-temperature limit is difficult to reach [25].

We thank Masud Haque, Jani Martikainen, and Nigel Cooper for helpful discussions. This work is supported by the Stichting voor Fundamenteel Onderzoek der Materie (FOM) and the Nederlandse Organisatie voor Wetenschappelijk Onderzoek (NWO).

---

[1] N.K. Wilkin, J.M.F. Gunn, and R.A. Smith, Phys. Rev. Lett. **80**, 2265 (1998); N.K. Wilkin and J.M.F. Gunn, Phys. Rev. Lett. **84**, 6 (2000).
[2] N.R. Cooper, N.K. Wilkin, and J.M.F. Gunn, Phys. Rev. Lett. **87**, 120405 (2001).
[3] T.-L. Ho and E.J. Mueller, Phys. Rev. Lett. **89**, 050401 (2002).
[4] B. Paredes, P. Zoller, and J.I. Cirac, Phys. Rev. A **66**, 033609 (2002).
[5] N. Regnault and Th. Jolicoeur, Phys. Rev. Lett. **91**, 030402 (2003).
[6] J. Sinova, C.B. Hanna and A.H. MacDonald, Phys. Rev. Lett. **89**, 030403 (2002).
[7] V. Schweikhard *et al.*, Phys. Rev. Lett. **92**, 040404 (2004).
[8] V. Bretin *et al.*, Phys. Rev. Lett. **92**, 050403 (2004).
[9] A.L. Fetter, Phys. Rev. A **64**, 063608 (2001).
[10] J.-P. Martikainen and H.T.C. Stoof, Phys. Rev. Lett. **91**, 240403 (2003).
[11] N.R. Cooper *et al.*, Phys. Rev. A **72**, 063622 (2005).
[12] J.R. Abo-Shaeer *et al.*, Science **292**, 467 (2001).
[13] K. W. Madison *et al.*, Phys. Rev. Lett. **84**, 806 (2000).
[14] V.K. Tkachenko, Zh. Eksp. Teor. Fiz. **50**, 1573 (1996) [Sov. Phys. JETP **23**, 1049 (1966)].
[15] I. Coddington *et al.*, Phys. Rev. Lett. **91**, 100402 (2003).
[16] G. Baym, Phys. Rev. Lett. **91**, 110402 (2003).
[17] T. Mizushima *et al.*, Phys. Rev. Lett. **92**, 060407 (2004).
[18] L. O. Baksmaty *et al.*, Phys. Rev. Lett. **92**, 160405 (2004).
[19] E.J. Mueller, Phys. Rev. A **69**, 033606 (2004).
[20] J. Kim and A. L. Fetter, Phys. Rev. A **70**, 043624 (2004).
[21] A. Aftalion, X. Blanc, and J. Dalibard, Phys. Rev. A **71**, 023611 (2005); A. Aftalion, X. Blanc, and F. Nier, Phys. Rev. A **73**, 011601 (2006).
[22] N. R. Cooper, S. Komineas, and N. Read, Phys. Rev. A **70**, 033604 (2004).
[23] E. B. Sonin, Phys. Rev. A **71**, 011603(R) (2005).
[24] F. Chevy, cond-mat/0511547.
[25] V. Schweikhard, private communication.